Tunable Microwave Load Based on Biased Photoinduced Plasma in Silicon

Bertrand Boyer, Jihad Haidar, Anne Vilcot, *Member, IEEE*, and Michel Bouthinon, *Member, IEEE*

***Abstract*—The frequency tuning of a quarter-wave resonator using an optoelectronic control is reported. Sharp notch characteristics with a small decibel-insertion loss and tunable frequency with matching better than 45 dB are obtained by varying both the optical power and the dc bias. The measured frequency shift is more than 60% below the dark resonant frequency and is carried out without altering the shape of the response. The biased photoinduced plasma (BPP) loading the open terminated microstrip line is then analyzed by comparing microwave simulations and measurements. The deduced complex load equivalent to this biased photoinduced plasma is then confirmed by semiconductor simulations. Results show the great possibilities offered by this BPP load (BPPL), which can be easily and widely tuned by means of a simple optoelectronic control. The frequency bandwidth of tuning is limited by the geometrical parameters and may be extended to millimeter-wave operation.**

***Index Terms*—Microwaves, optical control, photoconductivity, photo-induced load, silicon.**

I. Introduction

These days there is an increasing interest in the optical control of microwave devices [1], [2]. This technique offers attractive advantages such as high isolation between the controlling optical beam and the controlled microwave signal, fast response, and high-power handling capability. As concerns passive structures, this offers the possibility of new devices to the classical microwave ones, such as switches [3], [4], phase shifters [5], tunable filters [6], and tunable attenuators [7], with a control easier than the classical mechanical adjustments—when these adjustments are possible. More recently, the possibility to integrate the optical command in the microwave substrate also appeared [8], which gives the possibility of monolithic integration of both the controlling and controlled signals.

Recently, a new optoelectronic control has been proposed [9]. It is based on the biasing of an optically induced plasma loading an open terminated microstrip-line section. In this paper, we first show experimental results concerning the optoelectronic command of a microwave resonator formed by an inductively coupled open stub. The input reflection-coefficient magnitude presents sharp notch characteristics with low insertion loss (less than 5 dB) and a matching at the resonance frequency better than 45 dB. This resonant frequency is tuned by the optical power and the dc bias over a wide band ($\Delta f/f > 60\%$).

We must notice that to our knowledge the only electrical tuning of a stub in integrated circuits consists of a varactor, which enables variations of the resonant frequency of only a few percents at our working frequencies. The lower resonant frequency here covers the band 1–4 GHz, but limitations in operating frequency are only inherent to the geometrical parameters. This optical control may be applied to millimeter-wave range.

The aim of this paper is to provide a basic model of the biased photoinduced plasma load (BPPL), which enables all these performances. We show that a simple *RC*-series circuit is compatible with the experimental measurements. Finally, the origin of complex load between the strip and the ground plane is identified by solving semiconductor transport equations.

II. Experimental Measurements

The device-under-test (DUT) is realized in the microstrip technology. It consists of a quarter-wave resonator ($Z_c = 100$ Ω, $l = 7$ mm, $w = 50$ μm) inductively coupled to a 50-Ω characteristic impedance main transmission line ($l = 4$ mm, $w = 410$ μm) (see Fig. 1). The substrate of high resistivity ($\rho = 5400$ Ω·cm) provides low microwave losses, it is a 500-μm-thick, slightly p-type, single crystal silicon. The strips are made of 0.5-μm-thickness sputtered aluminum.

For the measurements under illumination, an argon laser beam ($\lambda = 0.513$ μm) coupled into a multimodal fiber has been used, providing an output optical power at its end not exceeding 500 mW. The fiber is illuminating the open end of the device with a spot of 100 μm of diameter. An HP 8510 network analyzer is used both to measure the input reflection coefficient S_{11} of the resonator and to bias the photoinduced plasma.

The dark rejection frequency of the resonator is $f_r =$ 4.2 GHz. We observe that the open-end illumination of the resonator leads to a change of the rejection frequency, but at the same time the rejection gets less sharp. In the same way, applying a positive dc bias between the strip and the ground plane induces the same behavior, provided the device is under illumination. This last requirement is easily justifiable since we deal with a passive structure insensitive to the dc-bias when the illumination is turned off.

Manuscript received May 12, 1996; revised May 14, 1997.

B. Boyer, A. Vilcot, and M. Bouthinon are with Laboratoire d'Electromagnétisme Microondes et Optoélectronique UMR 5530 Institut National Polytechnique de Grenoble (INPG) UJF-CNRS, 38 016 Grenoble Cedex 1, France.

J. Haidar was with Laboratoire d'Electromagnétisme Microondes et Optoélectronique UMR 5530 Institut National Polytechnique de Grenoble (INPG) UJF-CNRS, 38 016 Grenoble Cedex 1, France. He is now with the Centre National d'Etudes des Télécommunications (CNET), 92 225 Bagneux, France.

Publisher Item Identifier S 0018-9480(97)05988-7.

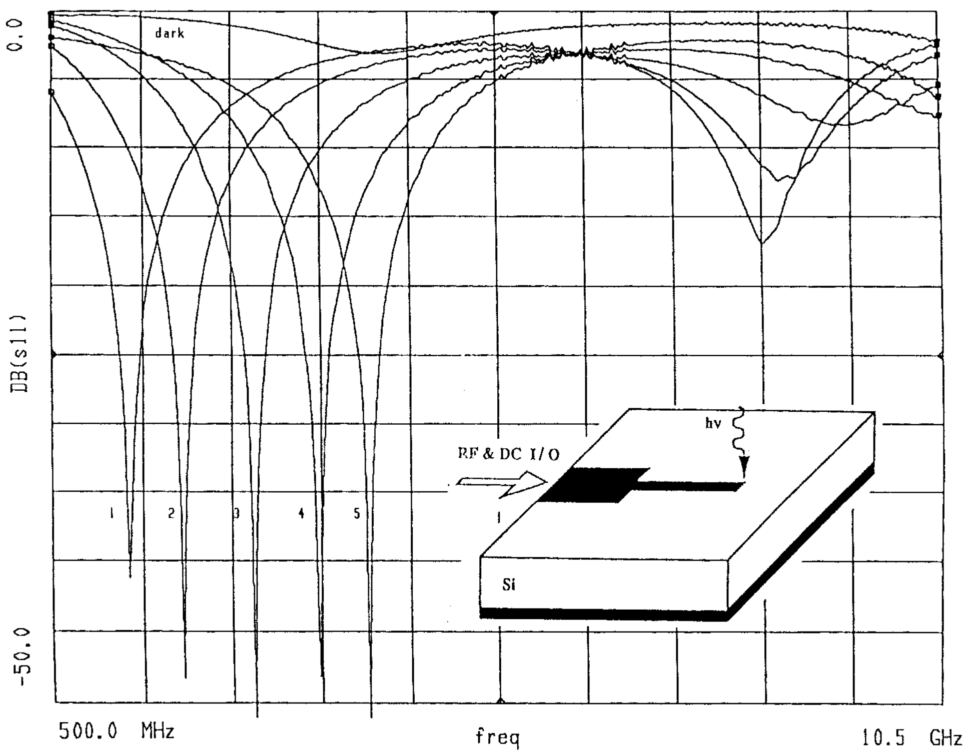

Fig. 1. Dark response and evolution of the rejection frequency for several couples (I, V) given in Table I. Schematic view of the microwave device.

Combining both the illumination (I) and the dc-bias (V) of the device enables the change of the resonator frequency, keeping a sharp rejection. In practice, for each optical power applied at the open end of the device, the tuning of the rejection frequency is obtained by adjusting the appropriate positive bias, showing a sharp rejection. Fig. 1 represents the magnitude of the reflection coefficient in decibels as a function of frequency for several couples of values (I, V) correctly chosen. An increase of the optical intensity leads to a decrease of the rejection frequency. For curve 1 corresponding to the maximum available optical power $I = 63$ W/mm^2, the dc bias is 10.8 V and the rejection frequency is the smaller ($f_1 = 1.33$ GHz). On the other side (curve 5), the highest resonant frequency ($f_5 = 4.025$ GHz) is obtained with the lower optical intensity ($I = 2.55$ W/mm^2) and a dc-bias of 0 V. This leads to a tuning of the rejection frequency with $(f_5 - f_1)/f_5 = 66\%$. Table I gives the resonant frequencies and the corresponding optical intensity and dc-bias values.

The second resonant frequency (around 9 GHz) can also be sharply tuned but with other values of both illumination and bias.

III. Intuitive Model

The purpose of this section is to provide a valuable explanation of the physical phenomena involved in the BPPL.

Considering that the incident photons have energies greater than the semiconductor band-gap energy, the illuminating light at the surface of the semiconductor is absorbed. This leads to the creation of electron–hole pairs and, thereby, locally increases the electron and hole concentrations in the semiconductor as well as the local conductivity at the end of the resonator. This can be thought of as a modification of the equivalent complex load at the end of the resonator. On one side, the resistance decreases from several megohms in the dark state, as the semiconductor has a high resistivity, to few ohms when the optical intensity increases. On the other side, the applied electric field modifies the injected carrier-density distribution and, as a consequence, both the resistivity and the depth penetration of the induced plasma change.

TABLE I
Performances of the BPPL and Its Model (R, C) at Each Couple (I, V)

Curve	I (W/mm^2)	DC bias (V)	f_r (GHz)	R (Ω)	C(fF)
1	63.66	10.80	1.33	39.9	2465.
2	38.20	15.10	1.95	56.6	1130.
3	15.91	17.00	2.75	100.	563.5
4	6.37	12.60	3.48	183.	480.8
5	2.55	0.00	4.03	234.	1909

The frequency change lies in the fact that the equivalent capacitance at the end of the resonator changes according to the bias and the optical intensity. We could imagine a metallic screw at the open end of the resonator (as it was done earlier) in microwave waveguides. When the optical intensity or the dc bias grows up, the screw plunges into the substrate and thus, the capacitance value between the screw and the ground plane changes.

Thus, the *first-order* equivalent model of the BPPL that we propose is serial resistance and capacitance. This model is confirmed both by microwave simulations and semiconductor considerations.

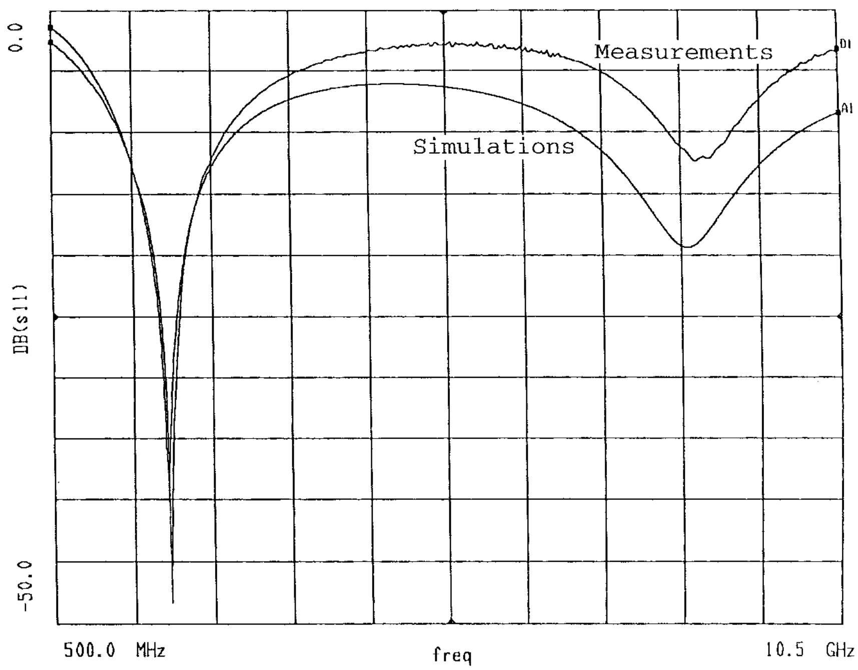

Fig. 2. Comparison between the MDS simulation results ($A1$) and the measurements ($D1$) for the device given in Fig. 1. $I = 38.2$ W/mm^2, $V = 15.1$ V.

IV. Microwave Simulations

The MDS software (Microwave Design System of Hewlett-Packard) has been used to simulate the response of the quarter-wave resonator shown in Fig. 1 when it is loaded by a *RC*-series circuit. The resistor and the capacitor values are calculated to have the same resonant frequency as the measurements. In Fig. 2, the comparison between the simulation results and the measurements shows good agreement on a large frequency range. For each couple of values (I, V) (intensity of illumination, bias), we associate a couple of values (R, C) that enables the fitting between the measurements and the simulations. Table I shows these coupled values (I, V) and (R, C) in correspondence.

This seems to confirm that at the first order the equivalent circuit of the BPPL is a *RC*-series circuit. Fig. 3 (the Smith chart) shows at $f = 2.5$ GHz, the variations of the (R, C) circuit equivalent to the BPPL for the (I, V) pairs given in Fig. 1, i.e., for values of (I, V) which enable a sharp rejection on this particular device. It is very interesting to note that any point of the lower half of the Smith chart (capacitive half) can be reached, provided adequate illumination and dc bias are applied on the device. This can be done by means of a simple optoelectronic tuning.

V. Semiconductor Considerations

In Section III, an intuitive model of the BPPL has been discussed, but semiconductor considerations can help in understanding more precisely the load created by photonics interaction. This section consists of a brief recollection of the semiconductor equations and a presentation of some results which confirm the previous model of the BPPL.

Three basic equations govern the semiconductor device, the Poisson's equation, and the two carrier continuity equations

$$\mathrm{div}(\varepsilon E) = \rho \tag{1}$$

where ε is the local permittivity, E is the electric field, and ρ is the local charge density

$$\frac{dn}{dt} = \frac{1}{q}\mathrm{div}(J_n) + G_n - R_n \tag{2}$$

$$\frac{dp}{dt} = -\frac{1}{q}\mathrm{div}(J_p) + G_p - R_p \tag{3}$$

where n and p are the electron and hole concentrations, J_n and J_p are the electron and hole current densities, G_n and G_p are the generation rates for electrons and holes, R_n and R_p are the recombination rates for electrons and holes, and q is the magnitude of the electron charge.

The first one gives the relation of the electrostatic field variation versus the local charge densities, and the two others describe the electron and hole density distributions based on transport, generation, and recombination processes.

To these three fundamentals equations, we add the relation between the electric field and the electrostatic potential: $E = -\mathrm{grad}V$, and the particular models for J_n, J_p, G_n, G_p, R_n, R_p.

The simplest model of the charge transport is the *drift-diffusion* model. The generation process is the optical generation, and the recombination is analyzed by several models: Schockley–Read–Hall, Auger, surface recombination. All these equations are taken into account in a semiconductor device simulator: Atlas of Silvaco, which has been used here to extract the equivalent circuit of the BPPL.

For better simplicity, a one-dimensional (1-D) resolution is operated. The device is a 1-μm-wide, 200-μm-long, and 500-μm-thick silicon block on which an aluminum line ($l = 50$

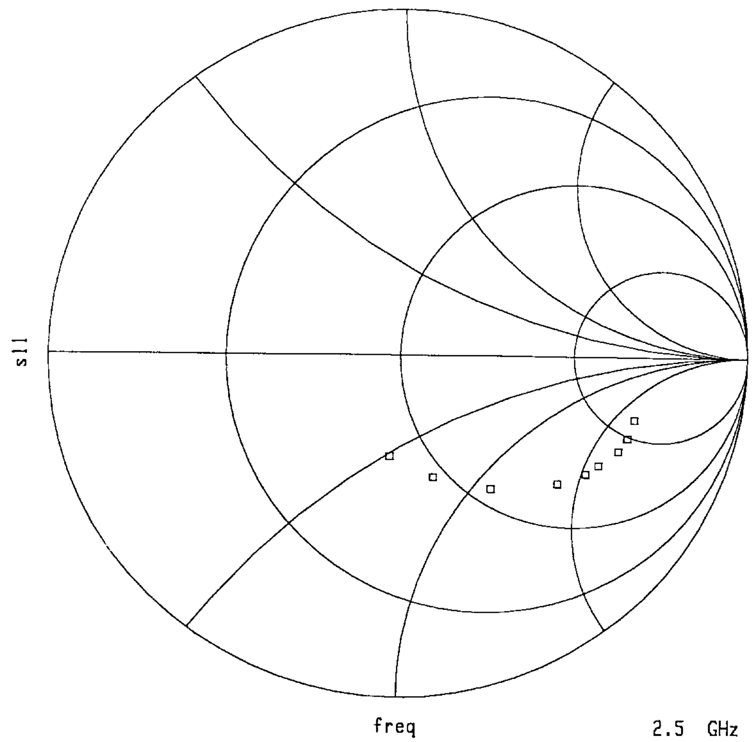

Fig. 3. Values of the (R, C) at $f = 2.5$ GHz, for various couples (I, V).

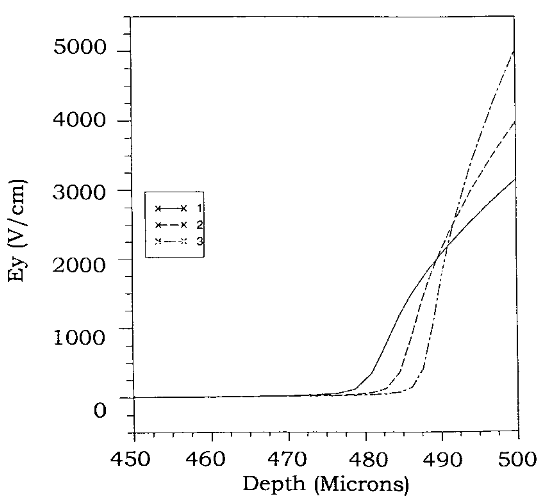

Fig. 4. Evolution of the electric field at the open end of the line as a function of depth for varying optical intensity and $V = 4$ V. 1: $I = 0.5$ W/mm^2, 2: $I = 1$ W/mm^2, 3: $I = 2$ W/mm^2.

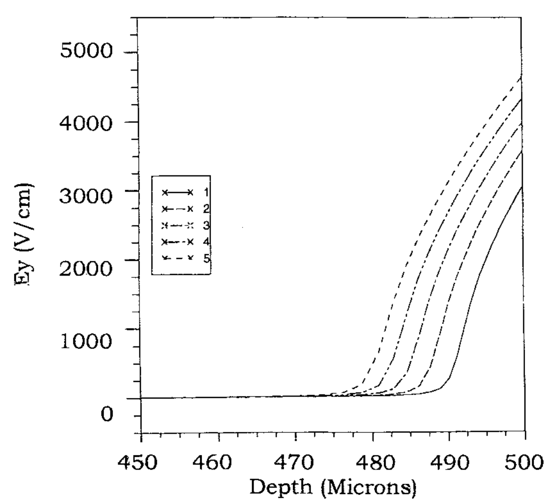

Fig. 5. Evolution of the electric field at the open end of the line as a function of depth for varying dc bias and $I = 1$ W/mm^2.1: $V = 2$ V, 2: $V = 3$ V, 3: $V = 4$ V, 4: $V = 5$ V, 5: $V = 6$ V.

μm) is deposited on the top, whereas the ground plane is made of aluminum on the backside. To compare with the experimental conditions, the component is illuminated by a laser ($\lambda = 0.513$ μm). Several dc biases and optical power simulations were performed.

The in-depth variation of the electrical-field E_y with the optical intensity as a parameter for a given dc bias is shown in Fig. 4 and with the dc-bias as a parameter for a given optical intensity shown in Fig. 5. These two figures indicate that two regions appear in the semiconductor submitted to both illumination and polarization. The first one, where the electric field is low, can be modeled by a resistor. The second one, where the electric fields grows up with the depth, can be modeled by a capacitor. When the optical power increases, electrons and holes concentration increase, i.e., the substrate becomes more conducting. If electrons and holes are more numerous, they will diffuse further. We can notice that the electrostatic energy is concentrated in less than 20 μm (to be compared to the 500-μm depth of the semiconductor substrate). This is possible because of the great lifetime of carriers in the Silicon ($\tau = 200$ μs). This leads to the image of the metallic screw which approaches the ground plane coming from the strip. As the electrostatic energy is concentrated in a small volume, the capacitance increases.

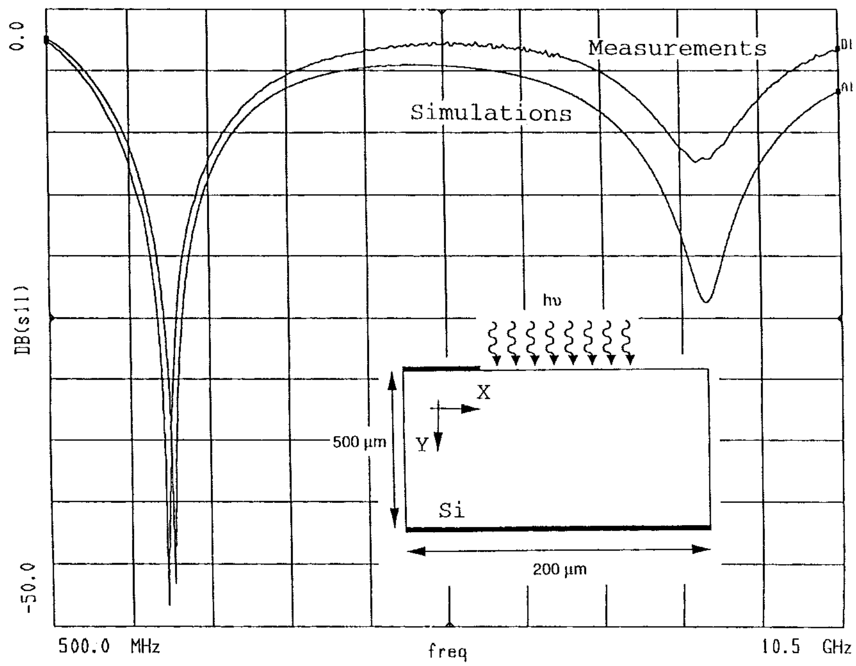

Fig. 6. Comparison between the Atlas simulations ($A1$) and the measurements ($D1$).

If we increase the dc bias, we notice that the penetration depth of the plasma changes, which is related to a variation of R, but this variation is weak. On the opposite, the electrical field increases, which induces a modification of C.

The semiconductor models provide a complex impedance value equivalent to the BPPL, varying with both optical intensity and bias. In brief, at the first order, the resistance R is governed by the optical intensity, while the capacitance C is controlled by both optical intensity and dc bias. All these observed interesting phenomena are probably related to the same order of the thickness of the substrate and the carrier diffusion length.

This impedance is then introduced in our MDS simulations as the load of the resonant device (shown in Fig. 1). The comparison between $S_{11}(f)$ obtained from the simulations and the measurements is shown in Fig. 6. Good agreement is obtained over a wide band of frequencies—especially around the resonant frequency, confirming once again the intuitive model.

VI. Discussion of the Results

The *RC*-series circuit given both by MDS and by Atlas fits very well with the measurements at low frequencies (Fig. 6). The mismatch at higher frequencies between the two curves can be explained by the use of a 1-D model for the first investigations on this phenomenon. This simple representation allows us to highlight the influence of each command, and is a good step in the understanding of the BPPL. To improve the model, we must use parallel *RC* elementary cells series-connected, which are obtained by discretizing the semiconductor depth, as in the case of simple optical control [10].

The diffusion length in the propagation direction is much less than the wavelength, thus enabling the validity of our model at the first order. Another improvement could be a resolution of the semiconductor equations in two or three dimensions. Hence, the lateral diffusion of holes and electrons will be taken into account. It may also be noticed that the semiconductor simulations are quasi-static equations. Although we apply a microwave signal, the model is still valid since the BPPL small dimensions are less than 10% of the wavelength (the width of the optical signal is approximately 100 μm). Thus, the BPPL is considered a lumped element.

VII. Conclusion

We have reported initial experimental investigations in which the resonant frequency of the resonator is tuned by an optoelectronic command over a wide band $(\Delta f/f > 60\%)$. The technique allows the tuning of open-stub-based microstrip structures. It is based on the biasing of a photoinduced plasma loading an open terminated microstrip line on silicon substrate. The presented experimental results show the importance which can have the BPPL in the easy tuning of open-stub-based resonators for variable frequency operation. The variations of the BPPL can be used not only to tune the resonant frequency of a resonator, but can also be useful in various kinds of microwave devices where tunable loads are needed.

We proposed a basic (first-order) model of this tunable microwave load confirmed by the resolution of semiconductor transport equations and verified by microwave simulations. We showed that the BPPL is equivalent at the first order to a *RC*-series circuit for our working frequencies. This load can be tuned over a wide area of the Smith chart, according to the dc bias and the optical intensity applied on the device.

This kind of load has the advantages of first being easily tuned and opening a door to a new generation of tunable devices, and secondly of being easily compatible with microwave integrated circuits.

Taking into account the fact that the equivalent capacitance of the BPPL varies in a nonlinear way according to either the dc-bias or the optical intensity, it can be used for mixing microwave frequencies, as is possible with varactors.

ACKNOWLEDGMENT

The authors would like to thank Dr. J. Boussey, researcher at the LPCS (Laboratoire de Physique des Composants à Semiconducteurs, Grenoble, France), for her precious help in understanding and using the Atlas software. They also wish to thank the technical staff of the CIME [Centre Interuniversitaire de MicroElectronique (INPG), Grenoble, France] and N. Corrao from the LHOG (Laboratoire d'Hyperfréquences et d'Optique Guidée, INPG, Grenoble, France) for their useful help during the preparation and characterization of the structures.

REFERENCES

[1] Special issue on applications of lightwave technology to microwave devices, circuits and systems, *IEEE Trans. Microwave Theory Tech.*, vol. 38, May 1990.
[2] Special issue on microwave and millimeter-wave photonics, *IEEE Trans. Microwave Theory Tech.*, vol. 43, Sept. 1995.
[3] D. H. Auston, "Picosecond optoelectronic switching and gating in silicon," *Appl. Phys. Lett.*, vol. 26, no. 3, pp. 101–103, Feb. 1975.
[4] C. H. Lee, "Picosecond optoelectronic switching in GaAs," *Appl. Phys. Lett.*, vol. 30, no. 2, pp. 84–86, Jan. 1986.
[5] P. Cheung, D. P. Neikirk, and T. Itoh, "Optically controlled coplanar waveguide phase shifters," *IEEE Trans. Microwave Theory Tech.*, vol. 38, pp. 586–594, May 1990.
[6] W. Platte, "Periodic-structure photoexcitation of a silicon coplanar waveguide for selective optoelectronic microwave control," *IEEE Trans. Microwave Theory Tech.*, vol. 38, pp. 638–646, May 1990.
[7] J. Haidar, A. Vilcot, and M. Bouthinon, "Optically tunable microwave attenuator using a quarter wave microstrip coupler," *Microwave Opt. Technol. Lett.*, vol. 10, no. 6, pp. 313–314, Dec. 20, 1995.
[8] S. Chouteau, J. Boussey, B. Cabon, and A. Illiadis, "Optoelectronic microswitch on SOI based structure," presented at the *1995 IEEE Int. SOI Conf.*, Tucson, AZ, Oct. 2–5, 1995.
[9] J. Haidar, M. Bouthinon, and A. Vilcot, "A new optoelectronic technique for microwave passive structures tuning," *1996 IEEE MTT-S Dig.*, San Francisco, CA, June 17–21, 1996, pp. 1437–1440.
[10] H. Shimasaki and M. Tsutsumi, "Reflection characteristics of optically-controlled microwave through an open-ended microstrip line," *EICE Trans. Electron.*, vol. E76-C, no. 2, pp. 301–304, Feb. 1993.

Bertrand Boyer was born in Reunion Island, France, in 1972. He received the agregation title in electronics from the Ecole Normale Supérieure of Cachan, France, in 1994, and the Diplome d'Etudes Approfondies from the Institut National Polytechnique de Grenoble (INPG), Grenoble, France, in 1995. He is currently working toward the Ph.D. degree in optics, optoelectronics, and microwaves at the INPG.

His research interests include the optical control of microwave devices, modeling, and the use of a photoinduced load in microwave devices on silicon substrates.

Jihad Haidar received the Ph.D. degree in optics, optoelectronics, and microwaves from the Institut National Polytechnique de Grenoble (INPG), Grenoble, France, in 1996.

In 1996, he joined the Centre National d'Etudes des Télécommunications (CNET), Bagneux, France, where he is currently working on polymer-based high-speed integrated electrooptic modulators. His research interests are in the field of optical and microwave interactions.

Anne Vilcot (S'90–M'92) received the engineer in electronics title from the Institut National Polytechnique de Grenoble (INPG), Grenoble, France, and the Diplome d'Etudes Approfondies in optics, optoelectronics, and microwaves from the INPG in 1989.

Since 1993, she has been an Associate Professor at the INPG, where she teaches courses on electromagnetism and microwaves. She is doing research with the microwave-photonics team on the optical control of microwave circuits.

Michel Bouthinon (M'89) received the "Docteur-ès-Sciences" degree from the University of Grenoble, Grenoble, France, in 1974.

In 1978, he became Professor at the University J Fourier of Grenoble, France, and has continued his research in the Laboratoire d'Electromagnétisme Microondes et Optoélectronique (LEMO) associated with the "Centre National de la Recherche Scientifique." Since 1992, he has been working on passive microwave components controlled by light. From 1986 to 1994, he was the Head of doctoral training in optics, optoelectronics, and microwaves common to two universities in Grenoble.